

Original Article

Comparison of Computed Tomography-Based Artificial Intelligence Modeling and Magnetic Resonance Imaging in Diagnosis of Cholesteatoma

Orkun Eroğlu¹ , Yeşim Eroğlu² , Muhammed Yıldırım³ , Turgut Karlıdag¹ , Ahmet Çınar⁴ ,
Abdulvahap Akyiğit¹ , İrfan Kaygusuz¹ , Hanefi Yıldırım² , Erol Keleş¹ , Şinasi Yalçın¹ 

¹Department of Otorhinolaryngology, Firat University, School of Medicine, Elazığ, Turkey

²Department of Radiology, Firat University, School of Medicine, Elazığ, Turkey

³Department of Computer Engineering, Malatya Turgut Özal University, Faculty of Engineering and Natural Sciences, Malatya, Turkey

⁴Department of Computer Engineering, Firat University, School of Engineering, Elazığ, Turkey

ORCID IDs of the authors: O.E. 0000-0001-9392-5755, Y.E. 0000-0003-3636-4810, M.Y. 0000-0003-1866-4721, T.K. 0000-0003-2748-7309, A.Ç. 0000-0001-5528-2226, A.A. 0000-0002-2192-155X, İ.K. 0000-0002-5237-2362, H.Y. 0000-0002-6204-6392, E.K. 0000-0003-4443-6714, Ş.Y. 0000-0002-6528-9234.

Cite this article as: Eroğlu O, Eroğlu Y, Yıldırım M, et al. Comparison of computed tomography-based artificial intelligence modeling and magnetic resonance imaging in diagnosis of cholesteatoma. *J Int Adv Otol.* 2023;19(4):342-349

BACKGROUND: In this study, we aimed to compare the success rates of computed tomography image-based artificial intelligence models and magnetic resonance imaging in the diagnosis of preoperative cholesteatoma.

METHODS: The files of 75 patients who underwent tympanomastoid surgery with the diagnosis of chronic otitis media between January 2010 and January 2021 in our clinic were reviewed retrospectively. The patients were classified into the chronic otitis group without cholesteatoma (n = 34) and the chronic otitis group with cholesteatoma (n = 41) according to the presence of cholesteatoma at surgery. A dataset was created from the preoperative computed tomography images of the patients. In this dataset, the success rates of artificial intelligence in the diagnosis of cholesteatoma were determined by using the most frequently used artificial intelligence models in the literature. In addition, preoperative MRI were evaluated and the success rates were compared.

RESULTS: Among the artificial intelligence architectures used in the paper, the lowest result was obtained in MobileNetV2 with an accuracy of 83.30%, while the highest result was obtained in DenseNet201 with an accuracy of 90.99%. In our paper, the specificity of preoperative magnetic resonance imaging in the diagnosis of cholesteatoma was 88.23% and the sensitivity was 87.80%.

CONCLUSION: In this study, we showed that artificial intelligence can be used with similar reliability to magnetic resonance imaging in the diagnosis of cholesteatoma. This is the first study that, to our knowledge, compares magnetic resonance imaging with artificial intelligence models for the purpose of identifying preoperative cholesteatomas.

KEYWORDS: Chronic otitis media, cholesteatoma, artificial intelligence, deep learning, CT, MRI

INTRODUCTION

The middle ear or other airy areas of the temporal bone may have stratified squamous keratinized epithelium, which is a condition known as cholesteatoma. It can also be defined histopathologically as a mass lesion made by desquamated epithelium and keratin, which is continuously produced by the ectopic basal germinative layer.¹ The annual incidence of acquired cholesteatoma ranges from about 9 to 12.6 cases per 100 000 adults and 3 to 15 cases per 100 000 children.² Anywhere in the temporal bone, including the middle ear, the mastoid air cells, and the petrous apex, cholesteatoma might develop. Cholesteatoma consequences can include meningitis, recurring infections, otorrhea, hearing loss (both sensorineural and conductive), facial nerve palsy, vertigo, tinnitus, otalgia, and headache. Its treatment is absolute surgery, and the frequency of recurrence after surgery varies between 5% and 15%.³

This study was presented at the 43th Turkish Otolaryngology and Head and Neck Surgery Congress, 16-20 November 2022, Antalya, Turkey.

Corresponding author: Orkun Eroğlu, e-mail: erogluorkun23@gmail.com

Received: November 29, 2023 • **Accepted:** February 27, 2023 • **Publication Date:** March 30, 2023

Available online at www.advancedotology.org



Content of this journal is licensed under a
Creative Commons Attribution-NonCommercial
4.0 International License.

Suspicion of cholesteatoma is formed by the patients' complaints, audiological examinations, and imaging techniques after physical examination, and the definitive diagnosis is made by postoperative histopathological examination. Even if the symptoms seem mild, cholesteatoma should be considered by clinicians because of the potentially dangerous complications. Recently, there have been significant changes in the management of cholesteatoma with radiological developments and the use of endoscopes in ear surgery. In the treatment of cholesteatoma, a patient-specific approach is required to suit the clinical and anatomical characteristics of each case, and recently, minimally invasive methods have been preferred as much as possible.⁴ Early detection of cholesteatoma enables the use of surgical techniques that are less intrusive than conventional therapies and can aid in the prevention of hearing loss, particularly in children. The importance of early diagnosis is increasing day by day in order to prevent the development of the mentioned potential complications and to treat cholesteatoma with minimal surgical approaches.

The most commonly used radiological imaging examinations in the preoperative diagnosis of cholesteatoma are high-resolution computed tomography and diffusion-weighted magnetic resonance imaging (DWMRI). Computed tomography is considered the first choice in middle ear imaging because of its high regional resolution and ability to identify important anatomical points.⁵ On CT, a decrease in aeration and bone erosions and an increase in soft tissue density are observed. It is not possible to distinguish cholesteatoma from otitis media, which is the most frequently confused clinical entity, and from other middle ear diseases, such as granulation tissue, fibrotic tissue, scar changes, and mucus secretions, only by CT. Diffusion-weighted magnetic resonance imaging is a very powerful tool for differentiating cholesteatoma from these middle ear pathologies with high sensitivity and specificity.^{6,7}

Despite the important contributions of radiological imaging in the diagnosis of cholesteatoma, there is still no technique that provides 100% preoperative diagnostic accuracy. In this sense, the imaging technique with the highest specificity and sensitivity is MRI. Recently, with the use of artificial intelligence in medicine, it has made an important contribution to clinicians in the diagnosis of many diseases. There is no study in the literature comparing the success rates of artificial intelligence and MRI in the diagnosis of preoperative cholesteatoma. In this study, we aimed to compare the accuracy of CT image-based artificial intelligence methods and MRI in the diagnosis of preoperative cholesteatoma.

MATERIAL AND METHODS

For the study, the files of patients who underwent mastoidectomy and/or tympanoplasty operation with the diagnosis of chronic otitis in our clinic between January 2010 and January 2021 were reviewed retrospectively. Computed tomography examination is routinely performed on patients diagnosed with chronic otitis in our clinic. In addition, an MRI examination is requested in cases with ear discharge resistant to medical treatment, ear pain, and suspected cholesteatoma during physical examination. In this way, primary patients who had both CT and MRI scans in our clinic and who had not been operated on for chronic otitis before were included in our study. The study was approved by the Non-Interventional Research Ethics Committee of Firat University (session date: 24.06.2021, number of sessions: 2021/08-21).

Patients who have undergone ear surgery for any reason, pediatric patients and cases of congenital cholesteatoma, patients without a follow-up record of at least 1 year following surgery, patients with disease recurrence in at least 1-year postoperative follow-up, patients with no discharge for at least 6 months, and patients whose middle ear mucosa is completely dry with only simple membrane are all excluded from our study. The study did not include patients with perforation and fully normal CT scans. Thus, 75 individuals with chronic otitis in total were included in the study. While intraoperative cholesteatoma was not encountered in 34 of these patients, cholesteatoma was observed during surgery in 41 of them. Cholesteatoma cases were 12 stage I, 24 stage II, 3 stage III, and 2 stage IV according to the EAONO/JOS classification.⁸ All cholesteatoma cases were acquired and were larger than 5 mm.

Creation of Groups for Artificial Intelligence Modeling

According to the presence of cholesteatoma during surgery, patients were classified into the chronic otitis group without cholesteatoma and the chronic otitis group with cholesteatoma. In order for artificial intelligence modeling to give more objective results, a control group was formed from 45 patients with normal CT images. The control group was formed from the images of patients who underwent CT and who were reported as normal based on the etiology of otalgia, etiology of vertigo, temporomandibular joint disease, and hearing loss. Accordingly, the groups created for the application of artificial intelligence modeling in our study are as follows: chronic otitis group without cholesteatoma (COM) (n=34), chronic otitis group with cholesteatoma (n=41), and the control group (n=45).

Then, preoperative computed tomography images of these patients were analyzed, and a CT dataset was prepared.

Computed Tomography Imaging Protocol

Multidetector CT images were acquired with 2 CT scanners (device 1: GE Healthcare, Optima CT660; Device 2: GE Healthcare, Revolution HD, Milwaukee, Wis, USA). Axial images of the temporal bone were obtained without the use of contrast material. Postprocessing coronal reformat images were created from these images. The imaging parameters were as follows for both devices: 120-140 kVp tube voltage; 240 mA tube current; exposure time 1.4 s; 0.625 mm section thickness; 25 cm field of view; 512 × 512 matrix size, and 0.531 pitch factor.

Preparation of Computed Tomography Dataset

Bone window adjustments were made for each patient on the axial and coronal plane images on the workstation (Enlil PACS Q/R server) [window level: 500 Hounsfield units (HU), window width: 3000 HU]. Then, datasets of our study groups were prepared by randomly recording 15-25 images in JPEG format containing diseased areas from each CT image. To produce a more uniform dataset, as many images of each subject as possible were acquired. The dataset was prepared by 2 otolaryngologists and 2 radiologists blindly, unaware of their primary diseases. Accordingly, in our study, 695 images were obtained from the chronic otitis group without cholesteatoma, 735 images from the chronic otitis group with cholesteatoma, and 845 images from the control group. Sample images of our patients are shown in Figure 1.

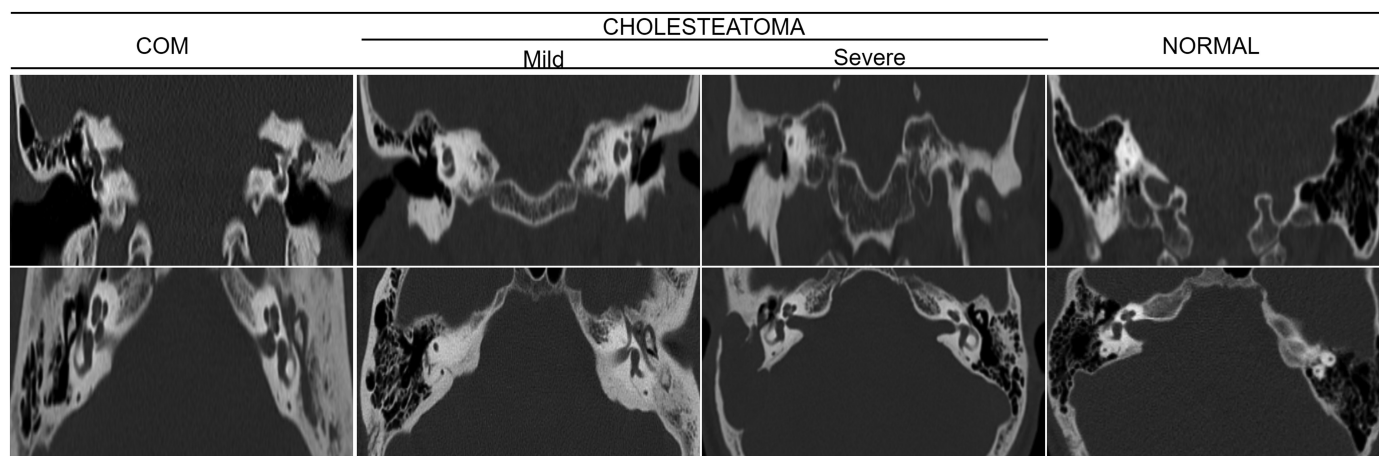


Figure 1. A few examples of the dataset's images.

Deep Models Used in the Study

Artificial intelligence refers to systems or machines that mimic human intelligence and can iteratively improve themselves based on the information they collect. The biggest feature of artificial intelligence systems is that they can process large amounts of data and obtain results from it. With the developing technology, different methods have been developed. After AlexNet architecture, one of the deep learning architectures, won the ImageNet Large Scale Visual Recognition Challenge (ILSVRC) ImageNet competition in 2012, deep learning architectures started to become more popular. The architectures used in this study are the ones accepted in the literature. The biggest difference between these architectures is that they consist of a different number of layers.

Deep learning architectures accepted in the literature were used to differentiate chronic otitis without cholesteatoma, chronic otitis with cholesteatoma, and normal images in the prepared dataset. Deep learning has been used in many areas with the development of technology in recent years. Deep learning has started to be used in many areas such as disease diagnosis and grading from biomedical images, recognition of human movements, the shopping and entertainment industry, face recognition, driverless cars, image classification, and video processing. There are different deep models accepted in the literature. At the core of these pre-trained deep learning models is training the models with training data and then testing the network with test data to measure the performance of the network.

Matlab 2021 was used to classify temporal CT images. In our study, 80% of the dataset's images were used for artificial intelligence applications' training, while 20% were used for testing. The results were obtained on a computer with an i7 processor and 8 GB of RAM. The models used in this study are AlexNet, GoogLeNet, MobileNetV2, ResNet50, DarkNet53, and DenseNet201.

AlexNet

Deep learning entered a new era with the AlexNet model, which won the 2012 ILSVRC ImageNet competition. After 2012, deep learning, which had a period of stagnation, started to gain popularity once more. Alex Krizhevsky, Ilya Sutskever, and Geoffrey Hinton created the AlexNet model. In the 2012 ImageNet ILSVRC competition, AlexNet architecture boosted classification accuracy from 74.3% to 83.6%. It is an extremely complex and potent model that utilizes

Graphics Processing Unit (GPU) technology. It reaches about 60 million parameter accounts.⁹ AlexNet architecture is designed to classify 1000 objects.

GoogLeNet

With an error rate of 6.66%, GoogLeNet won the ILSVRC ImageNet competition in 2014. This is one of the earliest models to abandon the sequential ordering of layers. In order to reduce the memory cost of the network and reduce the probability of the network memorizing, GoogLeNet has used modules connected in parallel instead of adding multiple layers on top of each other and using filters. These modules are called inception modules. Because of these modules, the GoogLeNet model has a more complex architecture than its predecessors.¹⁰

MobileNetV2

The MobileNet architecture is an architecture developed by Howard et al¹¹ in 2017. Researchers have developed this architecture to process lower datasets. Instead of using the standard convolution algorithm, this architecture made use of the depthwise separable convolution method. This method allows for feature extraction with 8-9 times less parameters than the conventional convolution procedure. Later, it was aimed to make the model faster and more efficient by making various updates in 2019.¹²

ResNet50

The ResNet model was developed by He et al¹³ in 2015. The ResNet model is the winning architecture of the ILSVRC ImageNet competition in 2015. The most important difference that distinguishes the ResNet model from the previous models is that it has a deeper structure. ILSVRC is a structure that came first with a 3.6% error rate in the competition held in 2015. It is one of the first algorithms to use batch normalization. This model, which has 26 million parameters, consists of 152 layers.

DarkNet53

DarkNet53 is a combination of DarkNet19 and ResNet in Yolov2. By making use of the experience of the ResNet network, the values in the past layers will be transmitted to the next layers more strongly. In this model, which consists of 75 layers, 53 convolution layers are used. Here, 1×1 and 3×3 filters are preferred. In the DarkNet53 architecture, stack normalization is preferred after almost every

convolution layer. After heap normalization, leakly ReLU was preferred.^{14,15}

DenseNet201

This architecture that Huang et al¹⁶ have developed is logically comparable to the ResNet model. However, rather than being added to other layers, the resultant activation functions are only combined. The original data are thus kept in all types of layers together with activations from earlier layers. Because of the shorter connections between layers in this architecture that are near to the input and output, it is claimed that this model is denser and more effective.

Magnetic Resonance Imaging Protocol and Imaging Analysis

Magnetic resonance images were obtained with Philips Healthcare, Ingenia, Netherlands device. The MRI sequences obtained in each patient were as follows: T1-weighted-turbo spin-echo (TSE) sequence, T2-weighted-TSE sequence, balanced-fast field echo sequence, diffusion-weighted imaging (DWI) sequence, and contrast-enhanced T1-weighted sequence. Two experienced radiologists were assigned to evaluate the MRIs of the patients included in our study. Diffusion-weighted imaging is an MRI sequence based on the movements of water molecules in tissues. This sequence is obtained with values that reflect the strength of diffusion, known as the *b* value. Cholesteatoma is diagnosed with typical high-signal features showing diffusion restriction on DWI.⁷

Diffusion-weighted imaging can be performed with echoplanar and non-echoplanar techniques. Echoplanar imaging (EPI) is the most popular DWI technique.¹⁷ Non-echoplanar imaging (non-EPI) has higher resolution and less artifact formation. Therefore, it can detect small-sized cholesteatomas with a higher success rate.¹⁸ It has been shown that non-EPI DWMRI detects cholesteatoma up to 2 mm in size with 91% sensitivity and 92% specificity.¹⁹ In a recent meta-analysis, it was reported that non-EPI DWI could be used for the diagnosis of cholesteatomas with a sensitivity and specificity of 94%.²⁰ Magnetic resonance imaging sequences show heterogeneity as the MRI protocols of the patients evaluated in our study have changed over the years. Due to the small number of patients in our study, only EPI or non-EPI evaluation was not performed, but MRI sequences were evaluated as a whole. In our study, radiologists, unaware of the clinical information of the patients, evaluated MRIs radiologically for the presence and absence of cholesteatoma. Patients with intraoperative cholesteatoma and diagnosed with cholesteatoma by preoperative MRI are true positive and patients with no cholesteatoma detected during surgery with cholesteatoma diagnosed during preoperative MRI are false positive. Cases without cholesteatoma detected during surgery and without cholesteatoma on preoperative MRI are true negative was determined as false negative in cases with intraoperative cholesteatoma but not diagnosed by preoperative MRI. In this

way, the success rate of MRI in the preoperative diagnosis of cholesteatoma was determined.

Accurate prediction rates in the diagnosis of cholesteatoma were recorded using artificial intelligence modeling in the dataset created from temporal CT images. The success rates of CT image-based artificial intelligence models and MRI were compared. The success rates of CT image-based artificial intelligence models and MRI were compared.

Statistical Analysis

The Statistical Package for the Social Sciences version 22.0 (IBM SPSS Corp.; Armonk, NY, USA) statistical program was used to analyze the data. Receiver operating characteristic analysis of the groups was performed. Performance evaluations of the artificial intelligence model were carried out on accuracy, specificity, and sensitivity metrics. In addition, the detection of cholesteatoma in surgery was accepted as the gold standard, and accuracy, specificity, and sensitivity values of cholesteatoma detection by MRI were calculated.

RESULTS

While pre-trained deep models were used in the study, the same training parameters were used in all models. Table 1 lists the training parameters utilized in these 6 different deep models.

Confusion matrices obtained from the models used in the study are given in Table 2.

It refers to 1—chronic otitis group without cholesteatoma, 2—chronic otitis group with cholesteatoma, and 3—control group.

Among the 6 pre-trained models we used to classify temporal CT images of chronic otitis media without cholesteatoma, chronic otitis with cholesteatoma, and normal groups in the prepared dataset, the lowest accuracy rate was obtained from the MobileNetV2, while the highest accuracy was obtained from the DenseNet201 architecture. When temporal CT images were classified using the MobileNetV2 architecture, 107 of the 139 COM images were correctly classified as COM, while 24 were classified as cholesteatoma and 8 were incorrectly classified as normal. Of the 147 cholesteatoma images of the MobileNetV2 architecture, 129 were correctly classified as cholesteatoma, 8 were classified as COM, and 10 were incorrectly classified. The same architecture correctly classified 143 of the 169 normal temporal CT images, while misclassifying 2 as COM and 24 as cholesteatoma. MobileNetV2 architecture correctly classified 379 of the 455 test images and misclassified 76 of them.

Table 1. Training Parameters of the Models

Models	Input Image Size	Minimum Batch Size	Maximum Epochs	Validation Frequency	Learning Rate
MobileNetV2	224 224 3	16	5	3	1e-4
GoogLeNet	224 224 3				
AlexNet	227 227 3				
DarkNet53	256 256 3				
ResNet50	224 224 3				
DenseNet201	224 224 3				

Table 2. Confusion Matrix of Deep Models

MobilenetV2				Googlenet				Alexnet						
True Class	1	107	24	8	True Class	1	109	19	11	True Class	1	118	10	11
	2	8	129	10		2	4	129	14		2	12	121	14
	3	2	24	143		3	1	26	142		3		8	161
		1	2	3			1	2	3			1	2	3
Predicted Class				Predicted Class				Predicted Class						

Darknet53				Resnet50				Densenet201						
True Class	1	119	18	2	True Class	1	118	3	18	True Class	1	123	7	9
	2	13	125	9		2	8	131	8		2	4	136	7
	3		13	156		3	8	9	152		3	6	8	155
		1	2	3			1	2	3			1	2	3
Predicted Class				Predicted Class				Predicted Class						

Table 3. Accuracy Metrics of Deep Models

MobileNetV2	GoogLeNet	AlexNet	DarkNet53	ResNet50	DenseNet201
83.30%	83.52%	87.91%	87.91%	88.13%	90.99%

The highest accuracy rate among the architectures used in the study in the classification of temporal CT images was obtained in the DenseNet201 architecture. When temporal CT images were classified using the DenseNet201 architecture, 123 out of 139 COM images were correctly classified as COM, while 7 were misclassified as cholesteatoma and 9 as normal. The DenseNet201 architecture correctly classified 136 of 147 cholesteatoma images as cholesteatoma, while 4 of them were classified as COM and 7 of them were misclassified. The same architecture correctly classified 155 of 169 normal temporal CT images and misclassified 6 as Com and 8 as cholesteatoma. The DenseNet201 architecture correctly classified 414 out of 455 test images and misclassified 41 of them.

The accuracy values obtained from the 6 architectures used in the study are given in Table 3.

When Table 3 is examined, the lowest accuracy rate was obtained in MobileNetV2 with 83.30%, while the highest accuracy rate was obtained in DenseNet201 with 90.99%. The performance values obtained in DenseNet201, where the highest accuracy value is obtained, are given in Table 4.

It was observed that 41 of the patients included in our study had cholesteatoma during surgery. Some of the patients had EPI DWIMRI

(n=27) and some had non-EPI DWIMRI (n=14). It was stated that 36 of these patients had cholesteatoma in the preoperative MRI, but it was stated by the radiologists that there was no cholesteatoma in 5 patients, although they had cholesteatoma during surgery. Magnetic resonance imaging evaluation of the patients is given in Table 5.

Table 4. Performance Values Obtained in the DenseNet201 Model (%)

	Accuracy	Sensitivity	Specificity	FPR	FDR	FNR	F1 Score
1	88.48	92.48	95.03	4.96	11.5	7.51	90.44
2	92.51	90.06	96.38	3.61	7.48	9.93	91.27
3	91.71	90.64	95.07	4.92	8.28	9.35	91.17

FDR, false discovery rate; FNR, false-negative rate; FPR, false-positive rate.

Table 5. Evaluation Between MRI and Surgical Findings

MRI	Surgery		Total
	Positive	Negative	
Positive	36	4	40
Negative	5	30	35
Total	41	34	75

MRI, magnetic resonance imaging.

Accordingly, the MRI accuracy was 88%, specificity was 88.23%, and sensitivity was 87.80% in our patient group.

DISCUSSION

Due to its potential complications, early diagnosis and treatment of cholesteatoma are very important in terms of increasing the quality of life. High-resolution computed tomography is still the most preferred imaging technique for cholesteatoma because it can show the middle ear anatomy in detail and identify important landmarks. Computed tomography can clearly show the extent of cholesteatoma and the extent of temporal bone invasion. However, fluid accumulation in the middle ear cannot fully demonstrate or exclude the presence of cholesteatoma due to mucosal edema and hypertrophy.²¹ Therefore, the sensitivity and specificity of CT in the diagnosis of cholesteatoma are low (70%).²² The sensitivity of CT in the diagnosis of postoperative cholesteatoma is 42.9% and its specificity is 48.3%, and it is quite limited.²³ In another study, it was reported that contrast-enhanced CT showed 75% diagnostic accuracy in the diagnosis of secondary cholesteatoma.²⁴

These low sensitivity and specificity rates in the diagnosis of cholesteatoma have led researchers to conduct different studies. The success of conventional MRI techniques in distinguishing cholesteatoma from other middle ear diseases is limited.²⁰ Diffusion-weighted imaging was first reported in 2002 by Maheshwari et al²⁵ who reported that it can be used for the diagnosis of residual cholesteatoma. Despite its low resolution and thick cross-sections, DWI was later reported as a very powerful diagnostic tool for the diagnosis of cholesteatoma.²⁶ Cholesteatoma contains a high content of keratin, and therefore cholesteatoma shows high signal intensity in DWI. Due to this feature, DWI has been frequently used in recent years by otolaryngologist to distinguish cholesteatoma from other middle ear diseases.

Recently, CT-DWMRI fusion studies have been carried out based on the idea of combining the high resolution of CT and the advantages of high specificity and sensitivity of MRI. It was emphasized that the diagnosis and localization of cholesteatoma could be determined more accurately with the fusion technique. With these advantages, good preoperative planning can be made for surgeons, and healthier preoperative information can be provided to patients.^{27,28} Another method used for the preoperative diagnosis of cholesteatoma is CT HU measurements. In a study, HU density was found to be statistically different between cholesteatoma and middle ear inflammatory tissue, and it was reported that HU measurements could be used to diagnose cholesteatoma with 51.2%–80.5% sensitivity and 80.5%–87.8% specificity.²⁹ It has been reported that it can be used in radiomics analyses to differentiate cholesteatoma and COM. Radiomics is the distinction between tissues based on the measurement of genetic, molecular, and biological properties of tissues and the signal intensity of gray area values in radiological images such as CT and MRI. Arendt et al³⁰ reported that in radiomics analysis using temporal CT images, the distinction between cholesteatoma and COM could be made with an accuracy rate approaching 90%.

With the artificial intelligence technology developed in recent years, image identification can be made and the diagnosis of diseases is made with the use of artificial intelligence in biomedicine. The diagnosis of numerous diseases, including brain tumors, breast

cancer, lung cancer, Alzheimer's disease, skin cancer, diabetic retinopathy, and stomach and colorectal lesions, has been studied in the literature using artificial intelligence models.^{31,32} With the use of artificial intelligence in medicine, studies have also begun in the field of otolaryngology. In a study in which autoendoscopic images were evaluated with artificial intelligence for the diagnosis of cholesteatoma, it was reported that cholesteatoma and inflammatory middle ear mucosa could be differentiated.³³ In a study in which artificial intelligence was used to differentiate cholesteatoma and COM using CT slices, it was reported that artificial intelligence predicted the diagnosis accuracy rate of 76.7%.³⁴ The highest correct prediction rate obtained with the artificial intelligence modeling used in our study was 90.99%, and a higher accuracy rate was achieved than their study.

In this study, we evaluated the preoperative temporal CT images of primary cholesteatoma cases operated in our clinic with artificial intelligence and compared the success rate of artificial intelligence in diagnosing with preoperative MRI. To our knowledge, there is no study in the literature comparing the success rates of MRI and artificial intelligence in the diagnosis of primary cholesteatoma. Our study is the first study in this field. According to the data we obtained, the correct diagnosis rate of primary cholesteatoma cases according to temporal CT-based artificial intelligence modeling was found as the lowest at 83.30% and the highest at 90.99%. The correct diagnosis rate of the same patients with preoperative MRI is 88%. According to the findings we obtained in our study, the preoperative correct diagnosis rate of artificial intelligence models (ResNet50 and DenseNet201) was found to be higher than MRI in the same patient group.

However, our study has some limitations. Due to the small number of patients in our study and the heterogeneity of the available MRI sequences, it could not be divided into groups such as EPI or non-EPI. We think that this may cause the MRI success rates to be slightly lower. Another limitation of our study is the small number of patients. Richer datasets can be created with more images to be obtained in studies with more patients. Thus, we think that the training of artificial intelligence models can be done at a higher level, and the correct diagnosis rates can be increased. In addition, only classical deep learning models were used in our study. It has been shown in the literature that higher accurate diagnosis rates can be obtained with hybrid models.³⁵ Another disadvantage of the method we proposed in our study is that it can only be used in primary cholesteatoma cases. No evaluation can be made for recurrence and revision cases. The patient groups in our study consisted of adult patients. Another limitation of our study is that we could not evaluate the performance of artificial intelligence in pediatric cases, congenital cholesteatoma cases, and cholesteatoma cases that were too small to cause any defect.

CONCLUSION

In conclusion, in this study, we showed that CT-based artificial intelligence modeling can provide a higher rate of accurate diagnosis than MRI in the diagnosis of preoperative cholesteatoma. Our method is not yet suitable for routine clinical practice. However, we think that artificial intelligence models that will be put into clinical practice with the developing technology over time will help the diagnosis of

cholesteatoma to be made more accurately and earlier, by reducing the workload of surgeons and radiologists. We also hope that artificial intelligence will be a very reliable alternative for diagnosing cholesteatoma in cases where MRI is not available or cannot be performed. Thus, cost and time loss will be avoided in terms of reducing the need for additional imaging examinations such as preoperative MRI. Additionally, using artificial intelligence for cholesteatoma diagnosis is highly quick and repeatable. In other words, modeling is more useful in the clinical situation when there is high diagnostic consistency. In addition, we aim to move our operations to the next segment by taking advantage of technological developments. In our next study, we want to increase the number of patients, develop an internet-based system, and reduce the burden on experts. We believe that the method we used in our study will contribute to the development of telemedicine in remote and rural areas where the number of specialist doctors is limited.

Ethics Committee Approval: Ethical committee approval was received from the Ethics Committee of Firat University (Session No: 2021/08-21, Date: June 24, 2021).

Informed Consent: N/A

Peer-review: Externally peer-reviewed.

Author Contributions: Concept – O.E., Y.E., M.Y.; Design – O.E., M.Y.; Supervision – T.K., A.C., H.Y., E.K.; Funding – A.A., İ.K., Ş.Y.; Materials – O.E., Y.E., M.Y., A.A.; Data Collection and/or Processing – O.E., Y.E., M.Y.; Analysis and/or Interpretation – O.E., M.Y., Y.E., T.K.; Literature Review – O.E., Y.E., M.Y., A.C.; Writing – O.E., Y.E., M.Y.; Critical Review – İ.K., E.K., Ş.Y., H.Y.

Declaration of Interests: The authors declare that they have no competing interest.

Funding: The authors declare that this study had received no financial support.

REFERENCES

1. An A. *Kulak Hastalıkları ve Mikrocerrahisi*. Ankara: Bilimsel Tıp Yayınevi; 1998:354-418.
2. Aquino JEAPd, Cruz Filho NA, de Aquino JN. Epidemiology of middle ear and mastoid cholesteatomas: study of 1146 cases. *Braz J Otorhinolaryngol*. 2011;77(3):341-347. [\[CrossRef\]](#)
3. Kerckhoffs KG, Kommer MB, van Strien TH, et al. The disease recurrence rate after the canal wall up or canal wall down technique in adults. *Laryngoscope*. 2016;126(4):980-987. [\[CrossRef\]](#)
4. Migirov L, Wolf M, Greenberg G, Eyal A. Non-EPI DW MRI in planning the surgical approach to primary and recurrent cholesteatoma. *Otol Neurotol*. 2014;35(1):121-125. [\[CrossRef\]](#)
5. Campos A, Mata F, Rebol R, Peris ML, Basterra J. Computed tomography and magnetic resonance fusion imaging in cholesteatoma preoperative assessment. *Eur Arch Otorhinolaryngol*. 2017;274(3):1405-1411. [\[CrossRef\]](#)
6. Corrales CE, Blevins NH. Imaging for evaluation of cholesteatoma: current concepts and future directions. *Curr Opin Otolaryngol Head Neck Surg*. 2013;21(5):461-467. [\[CrossRef\]](#)
7. Henninger B, Kremser C. Diffusion weighted imaging for the detection and evaluation of cholesteatoma. *World J Radiol*. 2017;9(5):217-222. [\[CrossRef\]](#)
8. Yung M, Tono T, Olszewska E, et al. EAONO/JOS joint consensus statements on the definitions, classification and staging of middle ear cholesteatoma. *J Int Adv Otol*. 2017;13(1):1-8. [\[CrossRef\]](#)
9. Krizhevsky A, Sutskever I, Hinton GE. Imagenet classification with deep convolutional neural networks. *Adv Neural Inf Process Syst*. 2017;60.
10. Szegedy C, Liu W, Jia Y, et al. Going deeper with convolutions. *IEEE Conference on Computer Vision and Pattern Recognition* 2015:1-9. [\[CrossRef\]](#)
11. Howard AG, Zhu M, Chen B, et al. Mobilenets: efficient convolutional neural networks for mobile vision applications. *arXiv Preprint ArXiv:170404861*. 2017.
12. Sandler M, Howard A, Zhu M, Zhmoginov A, Chen L-C. *MobileNetV2: Inverted Residuals and Linear Bottlenecks*. *IEEE/CVF Conference on Computer Vision and Pattern Recognition, USA*. 2018:4510-4520. [\[CrossRef\]](#)
13. He K, Zhang X, Ren S, Sun J. *Deep Residual Learning for Image Recognition*. *IEEE Conference on Computer Vision and Pattern Recognition, USA*. 2016:770-778. [\[CrossRef\]](#)
14. Moore D, Rid T. Cryptopolitik and the darknet. *Survival*. 2016;58(1):7-38. [\[CrossRef\]](#)
15. Kılıç B, Kablan EB, Doğan H, Ekinci M, Erçin ME, Ersöz Ş. Derin konvolüsyonel nesne algılayıcı ile plevral efüzyon sitopatolojisinde otomatik çekirdek algılama. *Türk Bilişim Vakfı Bilgisayar Bilimleri Mühendisliği Derg*. 2020;13(1):33-42.
16. Huang G, Liu Z, Van Der Maaten L, Weinberger KQ. *Densely Connected Convolutional Networks*. *IEEE Conference on Computer Vision and Pattern Recognition, USA*. 2017:2261-2269. [\[CrossRef\]](#)
17. Songu M, Altay C, Onal K, et al. Correlation of computed tomography, echo-planar diffusion-weighted magnetic resonance imaging and surgical outcomes in middle ear cholesteatoma. *Acta Otolaryngol*. 2015;135(8):776-780. [\[CrossRef\]](#)
18. van Egmond SL, Stegeman I, Grolman W, Aarts MC. A systematic review of non-echo planar diffusion-weighted magnetic resonance imaging for detection of primary and postoperative cholesteatoma. *Otolaryngol Head Neck Surg*. 2016;154(2):233-240. [\[CrossRef\]](#)
19. Lingam RK, Bassett P. A meta-analysis on the diagnostic performance of non-echoplanar diffusion-weighted imaging in detecting middle ear cholesteatoma: 10 years on. *Otol Neurotol*. 2017;38(4):521-528. [\[CrossRef\]](#)
20. Li PM, Linos E, Gurgel RK, Fischbein NJ, Blevins NH. Evaluating the utility of non-echo-planar diffusion-weighted imaging in the preoperative evaluation of cholesteatoma: A meta-analysis. *Laryngoscope*. 2013;123(5):1247-1250. [\[CrossRef\]](#)
21. Más-Estellés F, Mateos-Fernández M, Carrascosa-Bisquert B, Facal de Castro F, Puchades-Román I, Morera-Pérez C. Contemporary non-echo-planar diffusion-weighted imaging of middle ear cholesteatomas. *RadioGraphics*. 2012;32(4):1197-1213. [\[CrossRef\]](#)
22. Yiğiter AC, Pinar E, İmre A, Erdoğan N. Value of echo-planar diffusion-weighted magnetic resonance imaging for detecting tympanomastoid cholesteatoma. *J Int Adv Otol*. 2015;11(1):53-57. [\[CrossRef\]](#)
23. Tierney PA, Pracy P, Blaney SP, Bowdler DA. An assessment of the value of the preoperative computed tomography scans prior to otoendoscopic 'second look' in intact canal wall mastoid surgery. *Clin Otolaryngol Allied Sci*. 1999;24(4):274-276. [\[CrossRef\]](#)
24. Trojanowska A, Trojanowski P, Olszanski W, Klatka J, Drop A. Differentiation between cholesteatoma and inflammatory process of the middle ear, based on contrast-enhanced computed tomography imaging. *J Laryngol Otol*. 2007;121(5):444-448. [\[CrossRef\]](#)
25. Maheshwari S, Mukherji SK. Diffusion-weighted imaging for differentiating recurrent cholesteatoma from granulation tissue after mastoidectomy: case report. *AJNR Am J Neuroradiol*. 2002;23(5):847-849.
26. Vercruysse JP, De Foer B, Pouillon M, Somers T, Casselman J, Offeciers E. The value of diffusion-weighted MR imaging in the diagnosis of primary acquired and residual cholesteatoma: a surgical verified study of 100 patients. *Eur Radiol*. 2006;16(7):1461-1467. [\[CrossRef\]](#)

27. Lingam RK, Connor SEJ, Casselman JW, Beale T. MRI in otology: applications in cholesteatoma and Ménière's disease. *Clin Radiol*. 2018;73(1):35-44. [\[CrossRef\]](#)
28. Sharma SD, Hall A, Bartley AC, Bassett P, Singh A, Lingam RK. Surgical mapping of middle ear cholesteatoma with fusion of computed tomography and diffusion-weighted magnetic resonance images: diagnostic performance and interobserver agreement. *Int J Pediatr Otorhinolaryngol*. 2020;129:109788. [\[CrossRef\]](#)
29. Park MH, Rah YC, Kim YH, Kim JH. Usefulness of computed tomography Hounsfield unit density in preoperative detection of cholesteatoma in mastoid ad antrum. *Am J Otolaryngol*. 2011;32(3):194-197. [\[CrossRef\]](#)
30. Arendt CT, Leithner D, Mayerhoefer ME, et al. Radiomics of high-resolution computed tomography for the differentiation between cholesteatoma and middle ear inflammation: effects of post-reconstruction methods in a dual-center study. *Eur Radiol*. 2021;31(6):4071-4078. [\[CrossRef\]](#)
31. Eroglu Y, Yildirim M, Cinar A. mRMR-based hybrid convolutional neural network model for classification of Alzheimer's disease on brain magnetic resonance images. *Int J Imaging Syst Technol*. 2022;32(2):517-527. [\[CrossRef\]](#)
32. Çinar A, Yildirim M. Detection of tumors on brain MRI images using the hybrid convolutional neural network architecture. *Med Hypotheses*. 2020;139:109684. [\[CrossRef\]](#)
33. Miwa T, Minoda R, Yamaguchi T, et al. Application of artificial intelligence using a convolutional neural network for detecting cholesteatoma in endoscopic enhanced images. *Auris Nasus Larynx*. 2022;49(1):11-17. [\[CrossRef\]](#)
34. Wang YM, Li Y, Cheng YS, et al. Deep learning in automated region proposal and diagnosis of chronic otitis media based on computed tomography. *Ear Hear*. 2020;41(3):669-677. [\[CrossRef\]](#)
35. Eroğlu O, Eroğlu Y, Yıldırım M, et al. Is it useful to use computerized tomography image-based artificial intelligence modelling in the differential diagnosis of chronic otitis media with and without cholesteatoma? *Am J Otolaryngol*. 2022;43(3):103395. [\[CrossRef\]](#)